Sains Malaysiana 55(3)(2026): 475-489
http://doi.org/10.17576/jsm-2026-5503-10

Liver Metabolite Profiles and Oxidative Stress in Ageing Rats and Their Modulation by Tocotrienol-Rich Fraction

(Profil Metabolit Hati dan Tekanan Oksidatif pada Tikus yang Semakin Tua dan Modulasinya oleh Fraksi Kaya-Tokotrienol)

ANIKA TABASSUM[1], SITI LIYANA SAUD GANY[1], JEN KIT TAN[1,2] & SUZANA MAKPOL[1,2,*]

[1]Department of Biochemistry, Faculty of Medicine, Level 17 Preclinical Building, Universiti Kebangsaan, Malaysia, Jalan Yaacob Latif, Bandar Tun Razak, Cheras, 56000 Kuala Lumpur, Malaysia
[2]Ageing and Degenerative Diseases Research Group, Universiti Kebangsaan Malaysia, 43600 UKM Bangi, Selangor, Malaysia

Received: 25 September 2025/Accepted: 19 February 2026

ABSTRACT

Ageing alters liver metabolism and function, accompanied by morphological changes in hepatic cells, including disrupted metabolite profiles and structural degeneration. These changes contribute to increased oxidative stress and inflammation. However, the connection between oxidative stress, inflammation, histological changes, and liver metabolism during ageing, and the potential of the tocotrienol-rich fraction (TRF) as a therapeutic agent, remains underexplored. This study investigates age-related hepatic changes and the effects of TRF using metabolomics. Sprague-Dawley rats aged 3, 9, and 21 months were assigned to control and treatment groups and received either palm olein or TRF supplementation. Liver tissues were analysed using untargeted metabolomics via LC-MS/MS, along with histological evaluation and biochemical assessments of antioxidant enzymes (SOD, CAT), inflammatory markers (IL-6, TNF-alpha), and lipid peroxidation markers (MDA). SOD activity declined significantly with age in both control and TRF-treated old rats ($p<0.05$), suggesting reduced antioxidant defence with increasing age, whereas no significant changes were observed in CAT, IL-6 or MDA levels. Histologically, TRF-treated livers displayed fewer fibroblasts and less inflammation than control livers. Metabolomics showed age-related alterations in taurine and hypotaurine metabolism, pyrimidine metabolism (uridine and uracil), and TCA cycle components (malate and glutamate). These findings demonstrate that TRF modulates age-related liver changes, particularly in morphology and metabolism, despite a persistent decline in antioxidant activity. This finding underscores the potential of TRF in mitigating liver ageing. It provides insight into key metabolic pathways involved, offering a foundation for future therapeutic strategies targeting liver health in the elderly.

Keywords: Hepatic ageing; liver; metabolomics; oxidative stress; tocotrienol-rich fraction

ABSTRAK

Penuaan mendorong perubahan dalam metabolisme dan fungsi hati, disertai dengan perubahan morfologi dalam sel hepatik seperti profil metabolit yang terganggu dan degenerasi struktur. Perubahan ini menyumbang kepada peningkatan tekanan oksidatif dan keradangan. Walau bagaimanapun, hubungan antara tekanan oksidatif, keradangan, perubahan histologi dan metabolisme hati semasa penuaan dan potensi fraksi kaya-tokotrienol (TRF) sebagai agen terapeutik masih kurang diterokai. Penyelidikan ini mengkaji perubahan hepatik yang berkaitan dengan usia dan kesan TRF menggunakan pendekatan omik lanjutan. Tikus Sprague-Dawley berumur 3, 9 dan 21 bulan dibahagikan kepada kumpulan kawalan dan rawatan, menerima sama ada olein kelapa sawit atau suplemen TRF. Tisu hati dianalisis menggunakan metabolomik yang tidak disasarkan melalui LC-MS/MS, bersama-sama dengan penilaian histologi dan penilaian biokimia enzim antioksidan (SOD, CAT), penanda keradangan (IL-6,TNF-alpha) dan peroksidasi lipid (MDA). Aktiviti SOD merosot dengan ketara dengan umur dalam kedua-dua kawalan dan tikus yang dirawat TRF ($p<0.05$), mencadangkan pengurangan pertahanan antioksidan dengan peningkatan umur, manakala tiada perubahan ketara diperhatikan dalam tahap CAT, IL-6 atau MDA. Secara histologi, hati yang dirawat TRF menunjukkan lebih sedikit fibroblas dan kurang keradangan daripada hati kawalan. Metabolomik mendedahkan perubahan berkaitan usia dalam metabolisme taurin dan hipotaurin, metabolisme pirimidin (uridin dan uracil) dan komponen kitaran TCA (malat dan glutamat). Penemuan ini menunjukkan bahawa TRF memodulasi beberapa aspek perubahan hati yang berkaitan dengan usia, terutamanya dalam morfologi dan metabolisme, walaupun penurunan antioksidan yang berterusan. Hasil kajian ini menggariskan potensi TRF dalam mengurangkan penuaan hati dan memberikan gambaran tentang laluan metabolik utama yang terlibat, menawarkan asas untuk strategi terapeutik masa hadapan yang menyasarkan kesihatan hati dalam kalangan warga tua.

Kata kunci: Fraksi kaya-tokotrienol; hati; metabolomik; penuaan hepatik; tekanan oksidatif;

INTRODUCTION

Ageing is a complex process that causes functional changes from cells to organs, leading to declining health and an increased incidence of age-related illnesses (Guo et al. 2022). The rapidly growing ageing population has driven up healthcare costs, with age positively linked to expenditure (Rudnicka et al. 2020). Several theories contribute to the understanding of ageing, including the free radical theory, which categorises ageing into two main categories: alterations resulting from cellular damage and functional decline (Sobhon, Savedvanich & Weerakiet 2023). Accumulation of reactive oxygen species, ROS, damages cellular components, with free radicals driving degenerative changes in ageing (Militello et al. 2024). Oxidative stress, caused by excess ROS and weak antioxidant defence, damages lipids, proteins, and DNA, driving ageing and related diseases.

The liver, due to its crucial role in detoxification and metabolism, is particularly susceptible to oxidative damage (Chatterjee et al. 2025). Excess ROS induces lipid peroxidation, resulting in the production of aldehydes, such as malondialdehyde (MDA) (Gao et al. 2020). Additionally, ROS triggers the production of pro-inflammatory cytokines (IL-6, TNF-α), markers of liver injury and chronic inflammation (Kundu et al. 2020; Papatheodoridi et al. 2020). Because of its regenerative capacity, the liver has long been considered an organ that slows the ageing process (Chatterjee et al. 2025). However, the inevitable process of ageing is marked by a progressive decline in the liver's ability to metabolise substances effectively (Guo et al. 2022). Age-related changes in endothelial permeability impair the transport of metabolites (Czyzynska-Cichon et al. 2024). The ageing liver exhibits morphological changes, including lipofuscin accumulation, a marker of oxidative stress and fibrosis (Guo et al. 2022). Ageing limits liver regeneration through impaired proliferation, oxidative stress, and microvascular changes, thereby fostering the development of fibrosis and cirrhosis.

Metabolomic profiling is a key approach for biomarker discovery and tracking metabolic changes associated with ageing. Metabolomics shows age-related alterations in liver pathways and their links to oxidative stress and other physiological processes (Zhang et al. 2024).

As oxidative stress plays a central role in the ageing liver, antioxidant-based interventions have attracted significant research interest (Banerjee et al. 2023). Vitamin E, particularly in the form of tocotrienols, has emerged as a promising candidate owing to its strong antioxidant and anti-inflammatory activities (Atia, Salem Alra, et al. 2021; Mutalib et al. 2003). Palm oil serves as a rich source of tocotrienols and is often referred to as a tocotrienol-rich fraction (TRF) (Al-Baiaty et al. 2021). TRF supplements have been shown to promote healthy ageing, antioxidant properties and affect biochemical pathways (Md Shahrulnizam et al. 2024). Additionally, studies report that tocotrienols exhibit greater antioxidant potential than tocopherols, which has been attributed to their unsaturated isoprenoid side chain that facilitates deeper distribution (Maniam et al. 2008). Compared to tocopherols, they exhibit additional enhanced biological activities and antioxidant properties because of these unsaturated side chains, especially in terms of anti-inflammatory and cholesterol-lowering actions (Mutalib et al. 2003; Nakatomi et al. 2023). Accumulating evidence from experimental studies indicates that TRF exerts protective effects during ageing (Goon et al. 2024) against oxidative stress-induced hepatic injury. TRF enhanced endogenous antioxidant defences, reducing lipid peroxidation, preserving mitochondrial integrity, and modulating inflammatory signalling pathways (In Het Panhuis et al. 2023; Mathew et al. 2023).

Furthermore, advances in metabolomics have provided novel insights into age-related alterations in hepatic metabolism and the mechanisms by which TRF may exert its beneficial effects (Chin et al. 2011). Despite this growing body of evidence, a comprehensive synthesis of the mechanistic actions and experimental findings relating to TRF in liver ageing remains limited. The objectives of this study were to investigate age-related changes in liver metabolites in Sprague Dawley (SD) rats; to evaluate histological alterations and changes in oxidative stress, lipid peroxidation, and inflammatory markers in the liver during ageing; and to determine the modulatory effects of TRF on these hepatic changes. We hypothesised that metabolomic profiling would uncover age-related hepatic changes and that TRF supplementation would modulate them, indicating its potential to enhance liver health in ageing individuals. Thus, this research will contribute to a better understanding of the molecular mechanisms underlying age-related liver dysfunction with and without TRF.

MATERIALS AND METHODS

TRF TREATMENT

The RBD (refined, bleached, and deodorised) palm olein and TRF, tocotrienol-rich fraction (Golden Tri™ E 70), was provided by Sime-Darby Plantation Berhad (Kuala Lumpur, Malaysia). Each gram of TRF is made up of a mixture of vitamin E isomers, including 27% alpha-tocotrienol, 24% alpha-tocopherol, 4% beta-tocotrienol, 32% gamma-tocotrienol, and 14% delta-tocotrienol. RBD palm olein has an iodine content of 64.71%, 0.054% free fatty acids, 0.043% moisture and contaminants, and 0.45% peroxide values (Saud Gany et al. 2022). Each rat in the treated group received a dose of 60 mg of TRF per kilogram of body weight, and this treatment was administered continuously for 3 months (Saud Gany et al. 2022). Each week, 2.4 g TRF was mixed with 40 mL RBD palm oil, vortexed, wrapped in foil, and stored at 4 °C.

ANIMAL MODEL

Male Sprague Dawley (SD) rats, aged three, nine, and twenty-one months, were acquired from the Laboratory

Animal Resources Unit (LARU) at the Universiti Kebangsaan Malaysia (Saud Gany et al. 2022). Three age categories were established: young (3 months), adult (9 months), and old (21 months). Each group was further subdivided into control and treatment groups (n = 10 rats per group). Animals were housed individually in standard cages under controlled environmental conditions, with *ad libitum* access to food and water following a one-week acclimatisation period. Rats received the assigned treatment via oral gavage for three months. At the end of the treatment period, animals were euthanised, and livers were harvested, rinsed with 90% saline, and stored at -80 °C until further analysis. All animal procedures performed in this investigation were approved by the Universiti Kebangsaan Malaysia ethical committee under approval number BIOK/FP/2020/SUZANA/25-MAR/1099-MAR-2020-DEC.2022.

UNTARGETED METABOLOMICS ANALYSIS OF HEPATIC TISSUES

The chemicals used for metabolomics analysis were MS-grade unless specified otherwise. LC-MS with Folch extraction was used to analyse hepatic metabolites and assess the impact of TRF. Thawed liver tissue was homogenised in Milli-Q (MS) water at a ratio of 1 mL per g of tissue using a probe sonicator (QSonica). A total of 800 µL of methanol (MeOH) and 1 µL of internal standards (SPLASH LIPIDOMIX Mass Spec Standard, Avanti Research, Alabaster, AL, USA) were added to 100 µL of tissue lysate. The mixture was vortexed to ensure complete mixing, then 1.6 mL of dichloromethane (DCM) was added. After shaking (300 rpm, 1 h, RT), the mixture was supplemented with 600 µL water, vortexed, incubated for 10 min, then centrifuged (1,000 × g, 10 min, RT). The upper phase (1 mL) was collected and dried in a vacuum centrifuge (Eppendorf, Hamburg, Germany) at room temperature. The dried metabolite extracts were kept at -80°C until use. Dried polar extracts were reconstituted in 200 µL of 5% methanol and filtered through a 0.2 µm regenerated cellulose membrane syringe filter (Phenomenex, Torrance, CA, USA) into LC-MS vials with inserts. Quality control samples were prepared by pooling 10 µL from each sample, with the reconstitution buffer serving as the blank. Metabolomics data were acquired using LC-MS/MS on a UHPLC system (Dionex UltiMate 3000; Thermo Scientific, Torrance, CA, USA) coupled to an Orbitrap mass spectrometer (Q Exactive HF; Thermo Scientific) equipped with a heated electrospray ionisation (HESI) source, following a previously described method with slight modifications (Tan et al. 2023). Chromatographic separation was performed on a C18 column (2.1 mm ID × 100 mm L, 1.7 µm particle size, 100 Å pore size; Synchronis, Thermo Scientific) under the following conditions: column temperature 55 °C, autosampler temperature 10 °C, injection volume 2 µL, and flow rate 0.45 mL/min. Mobile phase A consisted of water with 0.1% formic acid, and mobile phase B was acetonitrile with 0.1% formic acid. The 22-minute gradient program was as follows: 0-1 min, 0.5% B; 1-16 min, linear increase to 99.5% B; 16-20 min, held at 99.5% B; and 20-22 min, returned to 0.5% B. The HESI source was operated with the following parameters: sheath gas flow 50 arbitrary units (AU), auxiliary gas flow 18 AU, sweep gas flow 0 AU, capillary temperature 320 °C, S-lens RF level 55 %, auxiliary gas heater temperature 300 °C, and spray voltage 3.5 kV (positive mode) and 3.0 kV (negative mode). Data were acquired using Xcalibur software (v4.2.47). QC samples were run at the start, every six injections, and at the end, with randomised sample order to balance groups. A coefficient of variation (CV) cutoff of <30% was applied to QC samples to ensure data robustness. Statistical analyses were carried out using MetaboAnalyst 5.0 (Pang et al. 2024, 2021). Data were normalised by log transformation and auto-scaling. PCA was employed to visualise sample distribution, and differentially expressed metabolites (DEMs) were identified using ANOVA, with significance defined as $p < 0.05$. Pathway analysis was also performed using MetaboAnalyst 5.0.

HEPATIC HISTOPATHOLOGY

Rat liver tissue samples from both control and treatment age groups were placed in plastic cassettes and fixed in 10% neutral buffered formalin at room temperature for 24 h. Following fixation, a tissue sample measuring approximately 1 × 1 cm was excised. Tissue processing and sectioning were performed using an automated tissue processor (Leica ASP200 S, Wetzlar, Germany). Sections were stained with Haematoxylin and Eosin (H&E) and examined under a light microscope at various magnifications.

HEPATIC ANTIOXIDANT ACTIVITY ASSAYS

Superoxide dismutase (SOD) and catalase (CAT) were selected as representative antioxidant enzymes due to their central roles in the enzymatic defence against reactive oxygen species. SOD catalyses the dismutation of superoxide radicals into hydrogen peroxide, which is subsequently converted to water and oxygen by CAT, reflecting the liver's antioxidant response. These enzymes were measured to assess oxidative stress levels associated with ageing and the potential modulatory effect of TRF. Liver homogenates were prepared as follows: 0.15 g of tissue in 1.5 mL of ice-cold phosphate-buffered saline (PBS; 50 mM, pH 7.4) was homogenised (10% w/v) and centrifuged at 10,000 rpm at 4 °C for 10 min. The resulting supernatant was collected and used for subsequent assays. Catalase assay: 0.1 mL homogenate with H_2O_2 and PBS (test) or PBS alone (blank) was run for 3 min, and H_2O_2 decomposition was measured at 240 nm ($E = 36\ M^{-1}cm^{-1}$) (Ulla et al. 2017). The spectrophotometric measurement of SOD activity was based on the inhibition of the reduction of Nitro Blue Tetrazolium (NBT). Absorbance was measured at 560 nm (Asiwe et al. 2024).

HEPATIC INFLAMMATORY AND LIPID PEROXIDATION MARKERS

Hepatic inflammatory status was evaluated across age groups by measuring inflammatory marker levels in rat liver tissues from both control and TRF-treated groups. The concentrations of interleukin-6 (IL-6) and tumour necrosis factor-alpha (TNF-α) were quantified as indicators of hepatic inflammation. In addition to inflammatory markers, hepatic lipid peroxidation was assessed by measuring malondialdehyde (MDA) levels in liver tissues, which reflect the extent of oxidative damage to cellular lipids. MDA concentrations were quantified using commercially available ELISA kits (ELK Biotechnology, Wuhan, China) according to the manufacturer's instructions. All ELISA measurements were performed in duplicates to ensure analytical reliability.

STATISTICAL ANALYSIS

For data other than metabolomics, the mean ± standard deviation (SD) was used to present all data. GraphPad Prism version 8.0 (GraphPad Software, San Diego, CA, USA) was used for statistical analysis and data visualisation. The one-way analysis of variance (ANOVA) was used to compare the groups, and Tukey's post hoc test was used to determine the differences. A p-value less than 0.05 was considered statistically significant. Normality was assessed by visual inspection of Q–Q plots of the residuals generated before performing one-way ANOVA.

RESULTS

METABOLITES PROFILE AMONG VARIOUS AGE CATEGORIES IN THE CONTROL AND TREATMENT GROUPS

An unsupervised PCA was performed on all six experimental groups, including both young and old rats with and without TRF treatment. The PCA score plot (Figure 1(A)) illustrates the distribution and clustering patterns of metabolite profiles across all treatment and control groups and age categories. The two principal components analysis explained a cumulative variance of 54.9%, with PC1 (the first principal component) contributing 40.3% and PC2 (the second principal component) contributing 14.6%. Clear separation was observed between the young control (YC) and old control (OC) groups (Figure 1(B)). PCA also showed separation between the adult control (AC) and OC groups. PCA showed a clear separation between the AC and YC groups, indicating that older age significantly influences the liver metabolic profile. In contrast to the distinct separations among age-related control groups, the comparison between the treatment groups and their respective age-matched control groups showed partial overlap (Figure 1(C)). This pattern may suggest subtle to moderate alterations in metabolites induced by TRF treatment across different age groups in rats.

EFFECTS OF AGE ON THE DIFFERENTIALLY EXPRESSED LIVER METABOLITES

To investigate the impact of age on hepatic metabolite changes, control groups were compared among young, adult, and old groups (Table 1). A total of 111 metabolites were annotated from the combined positive and negative ionisation modes. Across the age control groups, a total of 13 metabolites were significantly altered: 10 between AC and YC, six between OC and YC, and three between OC and AC. In the AC vs YC comparison, taurine ((+3.27 fold change (FC)) were elevated in adult controls, whereas N-acetyl-α-glucosamine1-phosphate (-1.13 FC), 4-guanidinobutyric acid (-2.87 FC), glycoursodeoxycholic acid (-6.35 FC), trigonelline (-3.07 FC), acetylarginine (-6.26 FC), leucine/isoleucine (-7.83 FC), 2-(Methylamino) isobutyric acid (-1.86 FC), acetyl-β-methylcholine (-4.81 FC), and pipecolinic acid (-2.20 FC) were decreased in adult controls compared to young controls. These alterations suggest age-related shifts in metabolites in adult livers. In the OC vs YC group, uridine (-6.78 FC), N-acetyl-α-glucosamine1-phosphate (-1.73 FC), uracil (-3.82 FC), 4-guanidinobutyric acid (-2.53 FC), acetylarginine (-4.79 FC), and sedoheptulose 7-phosphate (-4.43 FC) were significantly decreased in old controls. In the OC vs AC comparison, glycoursodeoxycholic acid (7.36 FC) was elevated in old livers, while uridine (-3.68 FC) and taurine (-2.91 FC) decreased.

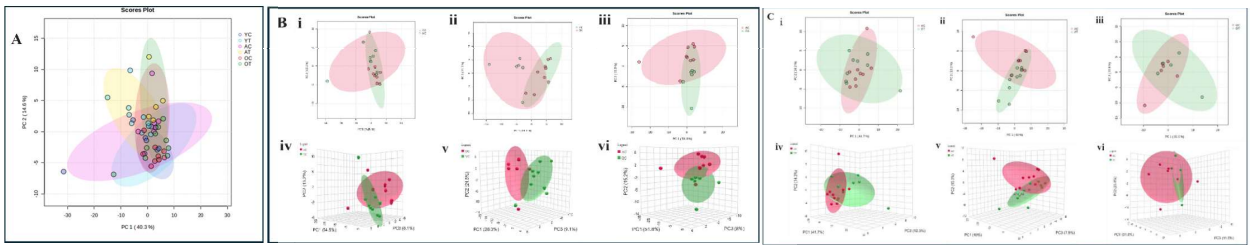

YC, young control; YT, young treatment; AC, adult control; AT, adult treatment; OC, old control; OT, old treatment

FIGURE 1. Distribution of samples for (A) all groups, (B) control groups between YC and AC (i, iv) YC and OC (ii, iv); AC and OC (iii, vi) and (C) treatment groups versus control groups between YT and YC (i, iv) AT and AC (ii, v); OT and OC (iii, vi) in PCA 2D and 3D score plots

EFFECTS OF TOCOTRIENOL-RICH FRACTION ON THE DIFFERENTIALLY EXPRESSED LIVER METABOLITES

Treatment groups were compared with their respective age-matched control groups; only the adult-treated (AT) vs AC showed significant metabolites. In contrast, no metabolites were significantly expressed in the young-treated (YT) versus YC and old-treated (OT) versus OC groups (Table 2). AT vs AC comparison identified 7 differentially expressed metabolites. All except one significantly altered metabolites in the AT group showed a decrease in relative to the AC group, including uridine (FC = -3.26), N-acetyl-α-glucosamine 1-phosphate (FC = -1.49), tryptophan (FC = -2.31), phenylalanine (FC = -3.20), glutamic acid (FC = -1.65), and malic acid (FC = -1.50). Conversely, acetyl-β-methylcholine showed a significant increase (FC = 3.90) in the AT group. These findings highlight specific metabolic responses to treatment in adult rats.

BIOCHEMICAL PATHWAYS OF DIFFERENTIALLY EXPRESSED METABOLITES IN THE LIVER OF CONTROL AND TREATMENT GROUPS

Biochemical pathway analysis of differentially expressed metabolites in the liver of control groups showed that taurine and hypo-taurine metabolism was a significant ($p < 0.05$) and impactful (impact value > 0.1) pathway in AC vs YC comparison (Figure 2(A), Supplementary Table 1). Other significant pathways in this comparison included valine, leucine and isoleucine biosynthesis. Pyrimidine metabolism was the significant pathway identified in OC vs YC (Figure 2(B), Supplementary Table 2). Two significant pathways were found in AT vs AC, i.e., glyoxylate and dicarboxylate metabolism, and nitrogen metabolism (Figure 2(C), Supplementary Table 3).

HEPATIC HISTOLOGICAL ANALYSIS

Hematoxylin and eosin (H&E) staining showed distinct morphological differences among the groups, indicating varying levels of structural integrity and cellular organisation in the liver tissues. YC liver sections displayed some fibrous cells, with relatively normal hepatocyte morphology and organisation. The tissue maintained a preserved cellular structure with minimal fibrotic changes. AC had a greater area with fewer cellular structures compared to the YT group. Fibroblast presence was more pronounced, suggesting increased fibrosis and extracellular matrix deposition. OC liver sections showed a smaller area with fewer cellular structures than AC. Hepatocytes appeared more elongated, indicating potential cellular stress or adaptation to ageing-related changes. In YT, hepatocyte arrangements were better than in the control, with improved cellular integrity and organisation. The liver tissue appeared structurally more preserved. In AT, there was a reduction in areas lacking cells compared to AC. The presence of fibroblasts was also lower, suggesting a possible protective or regenerative effect of the treatment. OT liver sections showed regions devoid of cells, with distinct morphological features compared with those of the younger groups. Fibroblast presence was reduced, and there were fewer migrated macrophages compared to OC,

TABLE 1. Significant liver metabolites in the control groups

Mode	Metabolites	ID	MW	RT	AC vs YC	OC vs YC	OC vs AC
-	Uridine	HMDB0000296	244.06	1.273	~	-6.77645	-3.68216
-	N-Acetyl-glucosamine 1-phosphate	HMDB0001367	301.05	0.544	-1.13252	-1.72989	~
+	Uracil	HMDB0000300	112.02	1.262	~	-3.82044	~
+	4-Guanidinobutyric acid	HMDB0003464	145.08	0.73	-2.87323	-2.52972	~
-	Glycoursodeoxycholic acid	HMDB0000708	449.31	8.912	-6.34679	~	7.3572
+	Taurine	HMDB0000251	125.01	0.53	3.2721	~	-2.9074
+	Trigonelline	HMDB0000875	137.04	0.656	-3.07825	~	~
+	Acetylarginine	HMDB0004620	216.12	0.785	-6.25821	-4.56934	~
+	Leucine/Isoleucine	HMDB0000678/HMDB0000172/ HMDB0013773	131.09	0.702	-7.83024	~	~
+	N-Methyl-a-aminoisobutyric acid	HMDB0002141	117.07	0.619	-1.863	~	~
-	Sedoheptulose 7-phosphate	HMDB0001068/HMDB0258206	290.03	0.532	~	-4.4342	~
+	Acetyl-β-methylcholine	HMDB0015654	159.12	0.923	-4.8151	~	~
+	Pipecolinic acid	HMDB0005960/HMDB0000070/ HMDB0000716	129.07	0.821	-2.20668	~	~

AC vs YC, where YC is set as a denominator; OC vs YC, where YC is set as a denominator; OC vs AC, where AC is set as a denominator. Tentative identification of liver metabolites was achieved by cross-referencing with the mzCloud database. (+) indicates increase; (-) indicates decrease. Acronyms: FC-fold change, MW-molecular weight, RT-retention time

suggesting an altered inflammatory or fibrotic response. These histological observations highlight age-related changes in liver architecture and the potential effects of treatment in maintaining tissue structure and reducing fibrotic alterations (Figure 3).

HEPATIC ANTIOXIDANT ENZYME ACTIVITY

The SOD activity varied significantly across different age and treatment groups (Figure 4(A)). In the control groups, young control rats exhibited significantly higher SOD activity than both adult and old control rats, indicating a natural decline in antioxidant defence mechanisms with ageing. A similar trend was observed across treatment groups by age: SOD activity was significantly higher in the young TRF-treated group than in the adult and old TRF-treated groups. CAT activity in the liver of SD rats was assessed across different age groups with and without TRF supplementation (Figure 4(B)). However, no significant differences in CAT activity were observed

TABLE 2. Significant liver metabolites in the TRF-treated groups

Mode	Metabolites	ID	MW	RT	YT vs YC	AT vs AC	OT vs OC
-	Uridine	HMDB0000296	244.06	1.273	~	-3.26339	~
-	N-Acetyl-glucosamine 1-phosphate	HMDB0001367	301.05	0.544	~	-1.49138	~
-	Tryptophan	HMDB0030396/HMDB0000929/ HMDB0013609	204.08	3.67	~	-2.31401	~
-	Phenylalanine	HMDB0250791	165.07	3.184	~	-3.19877	~
-	Glutamic acid	HMDB0000148/HMDB0003339/ HMDB0060475	147.05	0.526	~	-1.64968	~
+	Acetyl-β-methylcholine	HMDB0015654	159.12	0.923	~	3.9035	~
-	Malic acid	HMDB0000156/HMDB0031518	134.02	0.668	~	-1.50304	~

YC vs YT, where YC set as a denominator; AC vs AT, where AC set as a denominator; OC vs OT, where OC set as a denominator. Tentative identification of liver metabolites was achieved by cross-referencing with the mzCloud database.(+) indicates increase; (-) indicates decrease. Acronyms: FC-fold change, MW-molecular weight, RT-retention time

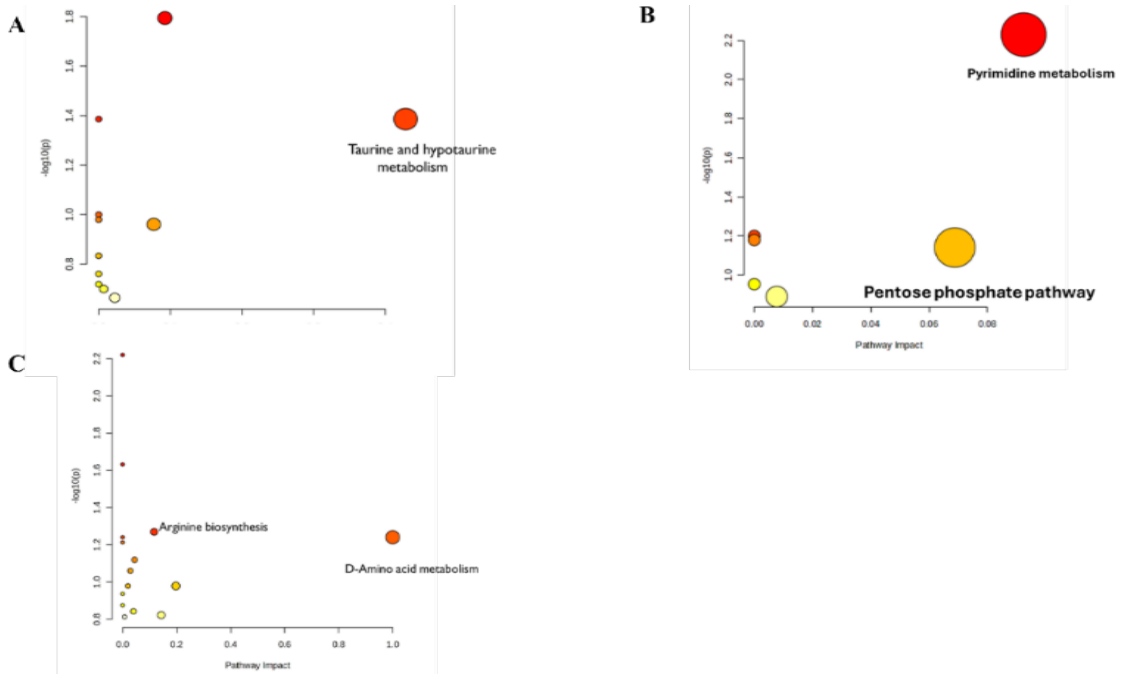

FIGURE 2. Metabolomic pathway analysis of significant metabolite profiles for (A) YC vs AC, (B) YC vs OC and (C) AT and AC groups

among the groups. This suggests that neither age nor TRF supplementation had a notable effect on catalase activity in the livers of SD rats under the conditions of this study.

HEPATIC INFLAMMATORY MARKERS LEVELS

The inflammatory cytokine IL-6 in the liver of SD rats was assessed across different age groups with and without TRF supplementation (Figure 5(A)). No significant differences were observed among the groups. This suggests that neither age nor TRF supplementation had a notable effect on IL-6 levels in the livers of SD rats. A similar trend was observed for the inflammatory cytokine TNF-alpha across groups, except that TNF-alpha levels were higher in the old TRF-treated group than in the young TRF-treated group (Figure 5(B)).

HEPATIC LIPID PEROXIDATION MARKER

The lipid peroxidation marker, MDA, in the ageing livers of SD rats with and without TRF treatment was measured (Figure 6). No significant differences were observed among the groups.

CORRELATION OF METABOLITES WITH OXIDATIVE, INFLAMMATORY AND LIPID PEROXIDATION MARKERS

The correlation heatmap shows the overall relationships among inflammatory markers (TNF-α, IL-6), antioxidant enzymes (SOD, CAT), and lipid peroxidation markers (MDA), regardless of age or treatment (Supplementary Figure 1). For SOD, several metabolites showed a positive correlation, indicating enhanced antioxidant defence. These included antioxidant and energy cofactors such as ergothioneine, flavin adenine dinucleotide (FAD), flavin mononucleotide (FMN), NAD^+, $NADP^+$, and oxidised glutathione, amino acids and derivatives including glutamic acid, glutamine, histidine, ornithine, and valine, and nucleotides/nucleosides such as guanosine monophosphate, uridine monophosphate, and inosine. In contrast, adenine and pyroglutamic acid (5-oxoproline) were negatively correlated with SOD, indicating reduced antioxidant activity associated with these metabolites. For IL-6, negative correlations were observed with several metabolites that overlapped with the SOD-positive profile. These included ergothioneine, FAD, FMN, glutamic acid, and glutamine, indicating that higher levels of these compounds are associated with lower inflammation and increased SOD activity. For MDA, positive correlations were primarily observed with adenine and pyroglutamic acid (5-oxoproline), which aligns with increased lipid peroxidation and oxidative stress. These metabolites represent potential markers of pro-oxidant states in the ageing liver. Although no significant correlation was observed when the groups were classified as control-only or treatment-only (Supplementary Figure 2), correlation analysis across individual age and treatment groups showed notable shifts in association patterns (Supplementary Figure 3). In the young control group, malic acid exhibited a significantly negative correlation with CAT. In contrast, in the adult control group, malic acid demonstrated a significantly positive correlation with CAT. This shift indicates an age-dependent modulation of malate metabolism in relation to catalase activity. In the adult control group, creatinine and stearamide were significantly and negatively correlated with TNF-α. Conversely, the correlation trends of these metabolites were significantly and positively correlated with TNF-α in the adult treated group. These findings suggest that TRF supplementation in adulthood may modulate these metabolites in response to inflammation.

DISCUSSION

Our study showed that dynamic metabolite changes occur in the liver during adulthood, particularly between YC and AC, and between AC and OC. N-acetyl-α-glucosamine-1-phosphate, sedoheptulose-7-phosphate, isoleucine, pipecolinic acid, uridine, uracil, 4-guanidinobutanoate, trigonelline, acetyl-arginine, methyl aminoisobutyric acid, and acetyl-β-methylcholine were seen to decrease with ageing liver, indicating that liver metabolism slows down with age. These metabolites are involved in various metabolic processes in the liver, including nucleotide, amino acid, and energy metabolism (Ling et al. 2023). Compared to young controls, adult rat livers exhibited altered taurine and hypotaurine metabolism, which is key to oxidative stress defence and lipid regulation (Guo et al. 2024). A critical metabolite in taurine and hypotaurine metabolism is taurine, whose levels were significantly higher in the adult control group than in the young and old control groups in this study. In acute liver failure, increased levels of hypotaurine and taurine correlate with decreased glutathione, potentially serving as an antioxidant mechanism (Mizota et al. 2021). Taurine is a non-essential amino acid synthesised in the liver from methionine and cysteine (Baliou et al. 2021). Taurine synthesis is influenced by GSH biosynthesis, as both require cysteine. In ethanol-induced liver injury, hepatic taurine levels increase (Hwang, Song & Kwon 2025). With age, there's a decrease in taurine biosynthesis that has been reported (Singh et al. 2023), as corroborated by the results of this study. These findings suggest elevated taurine and hypotaurine metabolism in adult liver may act as a compensatory defence against stressors. N-acetyl-α-glucosamine-1-phosphate (GlcNAc-1-P), a metabolite of the glycosylation pathway, declined with age, indicating altered sugar and energy metabolism. GlcNAc-1-P is a vital precursor to several glycosylation processes in the liver, such as N-glycosylation (Paneque et al. 2023), and the development of the man-6-P marker on lysosomal enzymes (Zhang et al. 2021), thus, slower protein glycosylation, which is crucial for liver function. Research on liver metabolism during ageing shows significant changes in energy and sugar metabolism (Petr et al. 2021). Age-related changes in enzyme activities

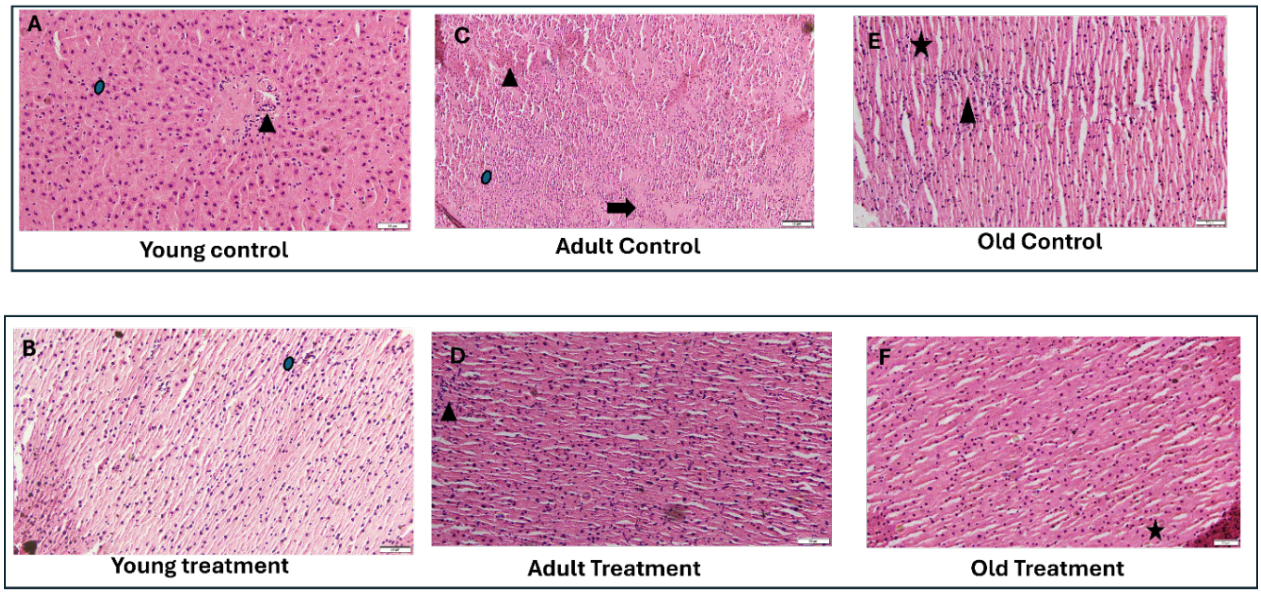

FIGURE 3. Histological differences in ageing liver tissues with and without TRF treatment (A) Young control - some fibrous cells are indicated, (B) Young treatment - shows some fibroblasts and arrangements are better than control, (C) Adult control - more area with fewer cell structures vs YT and fibroblasts are present, (D) Adult treatment - less area without cells, and with fewer fibroblasts, (E) Old control - less area of fewer cell structures, hepatocytes - structures are more elongated, and (F) Old treatment - more areas without cells, morphology different from young. Fewer fibroblasts or migrated macrophages vs OC

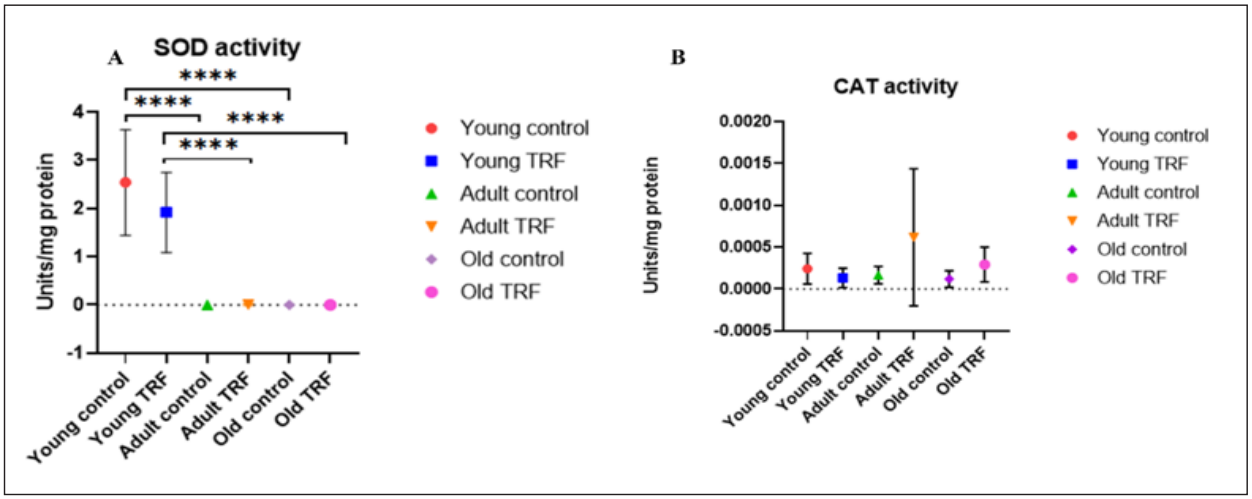

The *** indicates a significant difference of p = 0.0002 and **** indicates a significant difference of p <0.0001 according to the Tukey post-hoc test. Each bar represents the mean and SD, *n* = 8. Values are considered significance at p < 0.05. SOD activity is expressed in U/mg of protein. The activity of CAT is expressed in Units/mg, where Units is equal to µmol/mg of protein/min

FIGURE 4. (A) SOD and (B) Catalase activity in the liver of SD rats of different age group with and without TRF: young control (n=9), young TRF (n=9), adult control (n=9), adult TRF (n=10), old control (n=6d) and old TRF (n=5)

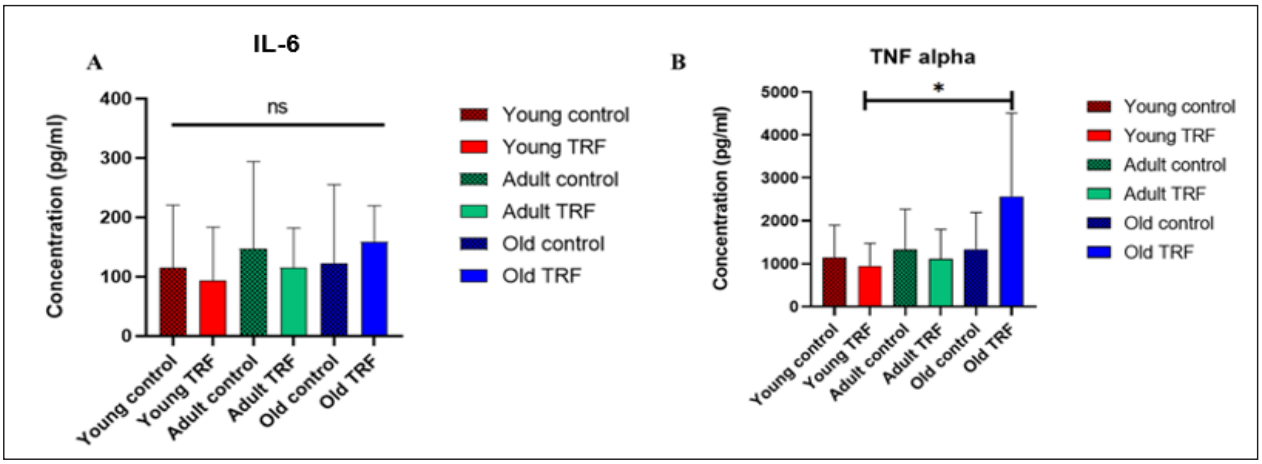

Data are shown in pg/mL. Each bar represents the mean and SD

FIGURE 5. Hepatic (A) IL-6 and (B) TNF- alpha levels were determined by enzyme-linked immunosorbent assay in the liver of SD rats of different age group with and without TRF: young control (n= 9), young TRF (n= 9), adult control (n= 9), adult TRF (n= 10), old control (n= 6), and old TRF (n=5)

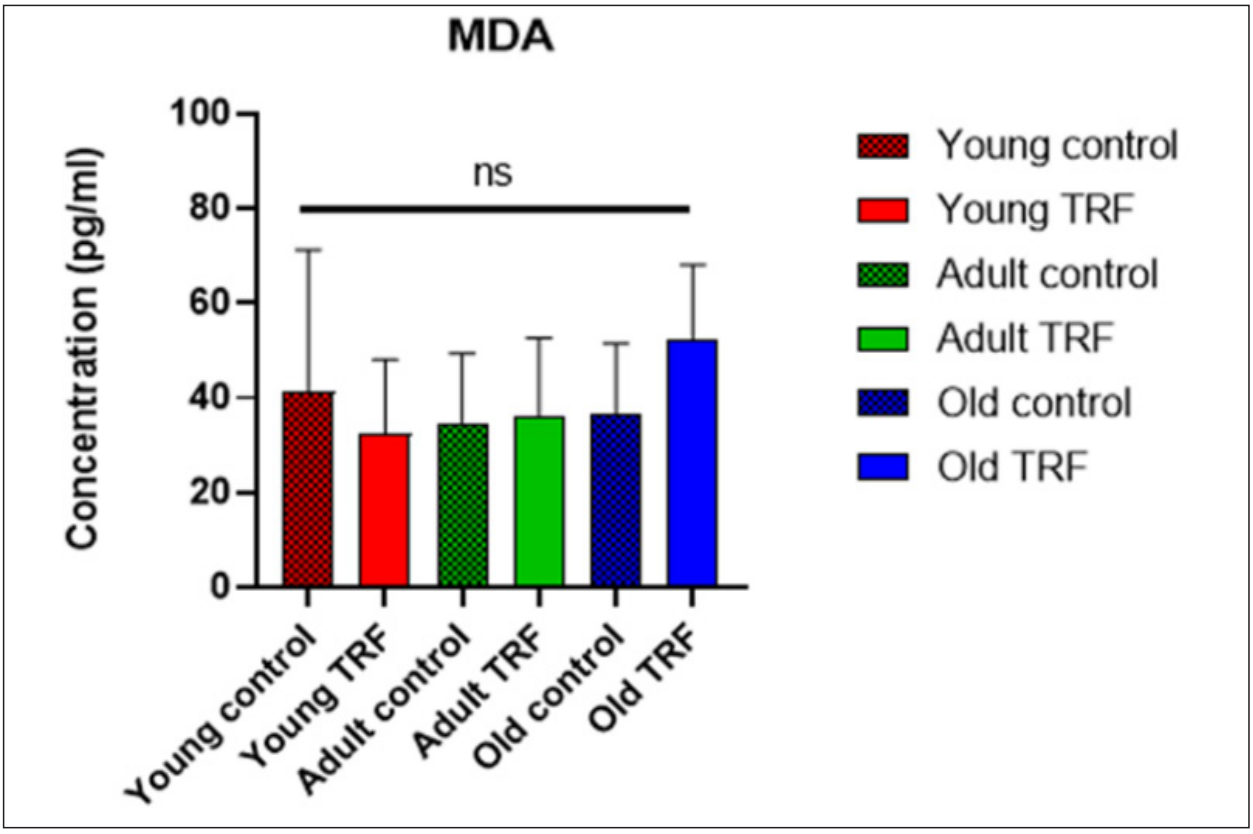

Data are shown in pg/mL. Each bar represents the mean and SD

FIGURE 6. Hepatic MDA levels were determined by enzyme-linked immunosorbent assay in the liver of SD rats of different age group with and without TRF: young control (n= 9), young TRF (n= 9), adult control (n= 9), adult TRF (n= 10), old control (n= 6), and old TRF (n=5)

and metabolite levels affect glycolysis and lipogenesis (Balashova et al. 2022). The alterations in sugar and energy metabolism, including changes in GlcNAc-1-P, contribute to the complex metabolic reprogramming observed in ageing livers. Ageing rat livers showed downregulation of uridine and uracil, indicating altered pyrimidine metabolism, consistent with previous findings linking ageing to changes in glutathione metabolism and immune function (Ekeuku et al. 2024). As uridine and uracil levels decrease with age, RNA synthesis also decreases in ageing livers (Xue et al. 2025). Additionally, the liver repair and cellular energy balance were disrupted in the livers of older rats. A decrease in uridine and uracil may indicate a slower hepatic regeneration in ageing. By generating bioactive intermediates and preserving suitable pyrimidine pools, the pyrimidine metabolism pathway plays a crucial biological role (Wang et al. 2021). Pyrimidine metabolism intermediates are essential biomolecules involved in the synthesis of DNA, lipids, and carbohydrates (Ekeuku et al. 2024). In our study, pyrimidine and β-alanine metabolism differed between young and old controls. In previous studies, we observed that uridine levels are altered in liver-related diseases (Xue et al. 2025). TRF supplementation was associated with significant metabolic alterations in adult rats, whereas no statistically significant metabolite changes were observed in the young or old groups, suggesting an effect on liver metabolic profiles during adulthood.

In our study, reduced glutamate signals a major metabolic shift in the liver after TRF treatment. Glutamate is a key amino acid involved in multiple metabolic pathways, and its reduction suggests increased utilisation for glutathione synthesis (Jin et al. 2023), supporting the antioxidant effects of TRF. This metabolomic shift likely affects several interconnected pathways, including glutathione metabolism, alanine, aspartate, and glutamate metabolism, as well as arginine biosynthesis, all of which rely on glutamate as a precursor or nitrogen donor (Holeček 2024). In liver fibrosis, the glutamine/glutamate ratio was disrupted, and glutamate and levels of TCA cycle intermediates increased as fibrogenesis progressed (Delgado, de las Heras & Martínez-Chantar 2022). Additionally, lower glutamate levels may influence nitrogen metabolism and the urea cycle, indicating a negative nitrogen balance (Luczkowska et al. 2024). This reduction also disrupts the metabolism of butanoate, histidine, and porphyrins, which are linked to energy regulation and oxidative stress (Wang et al. 2024). Correlation analysis of metabolites with other parameters across individual age and treatment groups showed notable shifts in association patterns, as shown in Supplementary Figures 1-3. In the adult-treated group, creatinine and stearamide showed positive correlations with TNF-α, whereas in adult controls, these correlations were negative. This shift suggests that TRF supplementation modulates the interaction of these metabolites with inflammatory pathways. One possible interpretation is that TRF induces metabolic remodelling in adults, altering the handling of lipids and energy metabolites in relation to cytokine activity. This may reflect a compensatory or adaptive response aimed at maintaining homeostasis, rather than a direct pro-inflammatory effect. Despite providing valuable insights into the hepatoprotective effects of TRF during ageing, this study has some limitations. Although untargeted metabolomics enabled broad identification of altered metabolic pathways, targeted validation of specific metabolites was not performed, which is essential to confirm biomarker relevance. In addition, the absence of transcriptomic or proteomic analyses limits deeper mechanistic understanding of the molecular pathways influenced by TRF. Furthermore, histological assessment was limited to H&E staining and general inflammatory markers, without fibrosis- or cell-type-specific staining, which could have provided more detailed structural and pathological characterisation.

CONCLUSIONS

TRF treatment showed beneficial effects by improving liver morphology and modulating age-associated metabolic disruptions, particularly in taurine and hypotaurine metabolism, pyrimidine metabolism, and energy-related pathways such as the TCA cycle. Overall, TRF supplementation was associated with metabolomic alterations in adult livers and histological differences across ageing livers, reflecting the metabolic and structural changes observed in this study. By combining metabolomics with histological and biochemical analyses, this study offers valuable insights into the molecular mechanisms of liver ageing. It highlights the therapeutic potential of TRF in mitigating age-related hepatic decline.

ACKNOWLEDGEMENTS

This study was funded by the Dana Impak Perdana grant DIP-2024-016 from Universiti Kebangsaan Malaysia.

REFERENCES

Al-Baiaty, F.D.R., Ismail, A., Abdul Latiff, Z., Muhammad Nawawi, K.N., Raja Ali, R.A. & Mokhtar, N.M. 2021. Possible Hepatoprotective Effect of Tocotrienol-Rich Fraction Vitamin E in Non-alcoholic Fatty Liver Disease in Obese Children and Adolescents. *Frontiers in Pediatrics* 9: 667247.

Asiwe, J.N., Yovwin, G.D., Alawode, M.O., Isola, T., Umukoro, E.K., Igbokwe, V.U. & Asiwe, N. 2024. Lutein protection against doxorubicin-induced liver damage in rats is associated with inhibition of oxido-inflammatory stress and modulation of Beclin-1/mTOR activities. *Naunyn-Schmiedeberg's Archives of Pharmacology* 398(5): 5811-5822.

Atia, A., Salem Alra, N. & Abdullah, A. 2021. Effect of Tocotrienol-Rich Fraction on Superoxide Dismutase 3 Expression in Mice Liver. *International Journal of Pharmacology* 17(8): 532–540.

Balashova, E.E., Maslov, D.L., Trifonova, O.P., Lokhov, P.G & Archakov, A.I. 2022. Metabolome profiling in aging studies. *Biology* 11(11): 1570.

Baliou, S., Adamaki, M., Ioannou, P., Pappa, A., Panayiotidis, M.I., Spandidos, D.A., Christodoulou, I., Kyriakopoulos, A.M. & Zoumpourlis, V. 2021. Protective role of taurine against oxidative stress. *Molecular Medicine Reports* 24(2): 605.

Banerjee, P., Gaddam, N., Chandler, V. & Chakraborty, S. 2023. Oxidative Stress–Induced Liver Damage and Remodeling of the Liver Vasculature. *The American Journal of Pathology* 193(10): 1400–1414.

Chatterjee, N., Sharma, R., Kale, P.R., Trehanpati, N. & Ramakrishna, G. 2025. Is the liver resilient to the process of ageing? *Annals of Hepatology* 30(2): 101580.

Chin, S.F., Ibahim, J., Makpol, S., Abdul Hamid, N.A., Abdul Latiff, A., Zakaria, Z., Mazlan, M., Mohd Yusof, Y.A., Abdul Karim, A. & Wan Ngah, W.Z. 2011. Tocotrienol rich fraction supplementation improved lipid profile and oxidative status in healthy older adults: A randomized controlled study. *Nutrition and Metabolism* 8(1): 1–14.

Czyzynska-Cichon, I., Kotlinowski, J., Blacharczyk, O., Giergiel, M., Szymanowski, K., Metwally, S., Wojnar-Lason, K., Dobosz, E., Koziel, J., Lekka, M., Chlopicki, S. & Zapotoczny, B. 2024. Early and late phases of liver sinusoidal endothelial cell (LSEC) defenestration in mouse model of systemic inflammation. *Cellular & Molecular Biology Letters* 29(1): 139.

Delgado, T.C., de las Heras, J. & Martínez-Chantar, M.L. 2022. Understanding gut-liver axis nitrogen metabolism in fatty liver disease. *Frontiers in Endocrinology* 13: 1058101.

Ekeuku, S.O., Ahmad Shahzalli, A.B., Tan, J.K. & Makpol, S. 2024. Untargeted metabolomic profiling on the effect of ginger on rat hepatic changes during ageing. *Journal of Functional Foods* 113: 106054.

Gao, H., Cao, Y., Xia, H., Zhu, X. & Jin, Y. 2020. CYP4A11 is involved in the development of nonalcoholic fatty liver disease via ROS-induced lipid peroxidation and inflammation. *International Journal of Molecular Medicine* 45(4): 1121-1129.

Goon, J.A., Ngah, W.Z.W., Makpol, S., Damanhuri, M.H.A., Ibrahim, N.F., Ghazali, N.I., Rais, R.Z.M., Chin, K.Y., Aminuddin, A., Yunus, M.H.M., Man, M.M., Neo, J.R.E., Loong, H.Y., Ung, Y.W. & Yap, W.N. 2024. A study protocol to assess the effectiveness of tocotrienol-rich fraction in older adults: A randomised, double-blind, placebo-controlled.

Guo, J., Huang, X., Dou, L., Yan, M., Shen, T., Tang, W. & Li, J. 2022. Aging and aging-related diseases: From molecular mechanisms to interventions and treatments. *Signal Transduction and Targeted Therapy* 7(1): 391.

Guo, X., Ou, T., Yang, X., Song, Q., Zhu, L., Mi, S., Zhang, J., Zhang, Y., Chen, W. & Guo, J. 2024. Untargeted metabolomics based on ultra-high performance liquid chromatography-mass spectrometry/MS reveals the lipid-lowering mechanism of taurine in hyperlipidemia mice. *Frontiers in Nutrition* 11: 1367589.

Holeček, M. 2024. Origin and roles of alanine and glutamine in gluconeogenesis in the liver, kidneys, and small intestine under physiological and pathological conditions. *International Journal of Molecular Sciences* 25(13): 7037.

Hwang, J., Song, Y. & Kwon, D. 2025. Impact of single ethanol administration following 12-hour fasting on hepatic sulfur-containing amino acid metabolism in mice. *Jeju Journal of Island Sciences* 2(1): 1-6.

In Het Panhuis, W., Schönke, M., Modder, M., Tom, H.E., Lalai, R.A., Pronk, A.C.M., Streefland, T.C.M., van Kerkhof, L.W.M., Dollé, M.E.T., Depuydt, M.A.C., Bot, I., Vos, W.G., Bosmans, L.A., van Os, B.W., Lutgens, E., Rensen, P.C.N. & Kooijman, S. 2023. Time-restricted feeding attenuates hypercholesterolaemia and atherosclerosis development during circadian disturbance in APOE∗3-Leiden.CETP mice. *EBioMedicine* 93: 104680.

Jin, E.S., Malloy, C.R., Sharma, G., Finn, E., Fuller, K.N.Z., Reyes, Y.G., Lovell, M.A., Derderian, S.C., Schoen, J.A., Inge, T.H. & Cree, M.G. 2023. Glycerol as a precursor for hepatic *de novo* glutathione synthesis in human liver. *Redox Biology* 63: 102749.

Kundu, D., Kennedy, L., Meadows, V., Baiocchi, L., Alpini, G. & Francis, H. 2020. The dynamic interplay between mast cells, aging/cellular senescence, and liver disease. *Gene Expression* 20(2): 77.

Ling, Z.N., Jiang, Y.F., Ru, J.N., Lu, J.H., Ding, B. & Wu, J. 2023. Amino acid metabolism in health and disease. *Signal Transduction and Targeted Therapy* 8(1): 1-32.

Luczkowska, K., Zhou, Y., Ramos-Lobo, A.M., Brun, T. & Maechler, P. 2024. Dietary protein load affects the energy and nitrogen balance requiring liver glutamate dehydrogenase to maintain physical activity. *Journal of Biological Chemistry* 300(7): 107473.

Mathew, A.M., Bhuvanendran, S., Nair, R.S. & K Radhakrishnan, A. 2023. Exploring the anti-inflammatory activities, mechanism of action and prospective drug delivery systems of tocotrienol to target neurodegenerative diseases. *F1000Research 2023 12:338* 12: 338.

Md Shahrulnizam, N.A.N., Mohd Efendy Goon, M.D., Ab Rahim, S., Lew, S.W., Sheikh Abdul Kadir, S.H. & Ibrahim, E. 2024. Palm-based tocotrienol-rich fraction (TRF) supplementation modulates cardiac sod1 expression, FXR target gene expression and tauro-conjugated bile acid levels in aleptinemic mice fed a high-fat diet. *Genes and Nutrition* 19(1): 1–11.

Militello, R., Luti, S., Gamberi, T., Pellegrino, A., Modesti, A. & Modesti, P.A. 2024. Physical activity and oxidative stress in aging. *Antioxidants* 13(5): 557.

Mizota, T., Hishiki, T., Shinoda, M., Naito, Y., Hirukawa, K., Masugi, Y., Itano, O., Obara, H., Kitago, M., Yagi, H., Abe, Y., Matsubara, K., Suematsu, M. & Kitagawa, Y. 2021. The hypotaurine-taurine pathway as an antioxidative mechanism in patients with acute liver failure. *Journal of Clinical Biochemistry and Nutrition* 70(1): 54.

Mutalib, M.S.A., Khaza'ai, H. & Wahle, K.W.J. 2003. Palm-tocotrienol rich fraction (TRF) is a more effective inhibitor of LDL oxidation and endothelial cell lipid peroxidation than α-tocopherol in vitro. *Food Research International* 36(5): 405–413.

Nakatomi, T., Itaya-Takahashi, M., Horikoshi, Y., Shimizu, N., Parida, I.S., Jutanom, M., Eitsuka, T., Tanaka, Y., Zingg, J.M., Matsura, T. & Nakagawa, K. 2023. The difference in the cellular uptake of tocopherol and tocotrienol is influenced by their affinities to albumin. *Scientific Reports 2023 13:1* 13(1): 1–11.

Paneque, A., Fortus, H., Zheng, J., Werlen, G. & Jacinto, E. 2023. The hexosamine biosynthesis pathway: Regulation and function. *Genes* 14(4): 933.

Pang, Z., Chong, J., Zhou, G., De Lima Morais, D.A., Chang, L., Barrette, M., Gauthier, C., Jacques, P.É., Li, S. & Xia, J. 2021. MetaboAnalyst 5.0: Narrowing the gap between raw spectra and functional insights. *Nucleic Acids Research* 49(W1): W388-W396.

Pang, Z., Lu, Y., Zhou, G., Hui, F., Xu, L., Viau, C., Spigelman, A.F., Macdonald, P.E., Wishart, D.S., Li, S. & Xia, J. 2024. MetaboAnalyst 6.0: Towards a unified platform for metabolomics data processing, analysis and interpretation. *Nucleic Acids Research* 52(W1): W398-W406.

Papatheodoridi, A.M., Chrysavgis, L., Koutsilieris, M. & Chatzigeorgiou, A. 2020. The role of senescence in the development of nonalcoholic fatty liver disease and progression to nonalcoholic steatohepatitis. *Hepatology* 71(1): 363-374.

Petr, M.A., Alfaras, I., Krawcyzk, M., Bair, W.N., Mitchell, S.J., Morrell, C.H., Studenski, S.A., Price, N.L., Fishbein, K.W., Spencer, R.G., Scheibye-Knudsen, M., Lakatta, E.G., Ferrucci, L., Aon, M.A., Bernier, M. & de Cabo, R. 2021. A cross-sectional study of functional and metabolic changes during aging through the lifespan in male mice. *ELife* 10: e62952.

Rudnicka, E., Napierała, P., Podfigurna, A., Męczekalski, B., Smolarczyk, R. & Grymowicz, M. 2020. The World Health Organization (WHO) approach to healthy ageing. *Maturitas* 139: 6-11.

Saud Gany, S.L., Tan, J.K., Chin, K.Y., Hakimi, N.H., Ab Rani, N., Ihsan, N. & Makpol, S. 2022. Untargeted muscle tissue metabolites profiling in young, adult, and old rats supplemented with tocotrienol-rich fraction. *Frontiers in Molecular Biosciences* 9: 1008908.

Sobhon, P., Savedvanich, G. & Weerakiet, S. 2023. Oxidative stress and inflammation: The root causes of aging. *Open Exploration* 4(2): 127-156.

Tan, J.K., Zakaria, S.N.A., Gunasekaran, G., Abdul Sani, N.F., Nasaruddin, M.L., Jaafar, F., Abu Bakar, Z.H., Amir Hamzah, A.I.Z., Nor Aripin, K.N., Mohd Rani, M.D., Noh, N.A., Damanhuri, H.A., Mazlan, M., Makpol, S. & Wan Ngah, W.Z. 2023. Metabolomics profiling of age-associated metabolites in Malay population. *Oxidative Medicine and Cellular Longevity* 2023(1): 4416410.

Ulla, A., Alam, M.A., Sikder, B., Sumi, F.A., Rahman, M.M., Habib, Z.F., Mohammed, M.K., Subhan, N., Hossain, H. & Reza, H.M. 2017. Supplementation of *Syzygium cumini* seed powder prevented obesity, glucose intolerance, hyperlipidemia and oxidative stress in high carbohydrate high fat diet induced obese rats. *BMC Complementary and Alternative Medicine* 17(1): 1-13.

Wang, J., Qiu, Z., Zeng, H., Tan, Y., Huang, Y., Luo, J. & Shu, W. 2024. Long-term consumption of purified water altered amino acid, fatty acid and energy metabolism in livers of rats. *Metabolites* 14(5): 289.

Wang, W., Cui, J., Ma, H., Lu, W. & Huang, J. 2021. Targeting pyrimidine metabolism in the era of precision cancer medicine. *Frontiers in Oncology* 11: 684961.

Xue, Q., Zhou, X., Wang, Y., Liu, Y., Li, X., Xiong, C., Liu, X. & Huang, Y. 2025. Mass spectrometry imaging reveals spatial metabolic variation and the crucial role of uridine metabolism in liver injury caused by *Schistosoma japonicum*. *PLOS Neglected Tropical Diseases* 19(2): e0012854.

Zhang, J., Wu, J., Liu, L. & Li, J. 2021. The crucial role of demannosylating asparagine-linked glycans in ERADicating misfolded glycoproteins in the endoplasmic reticulum. *Frontiers in Plant Science* 11: 625033.

Zhang, S., Wang, Z., Wang, Y., Zhu, Y., Zhou, Q., Jian, X., Zhao, G., Qiu, J., Xia, K., Tang, B., Mutz, J., Li, J. & Li, B. 2024. A metabolomic profile of biological aging in 250,341 individuals from the UK Biobank. *Nature Communications* 15: 8081.

*Corresponding author; email: suzanamakpol@ukm.edu.my

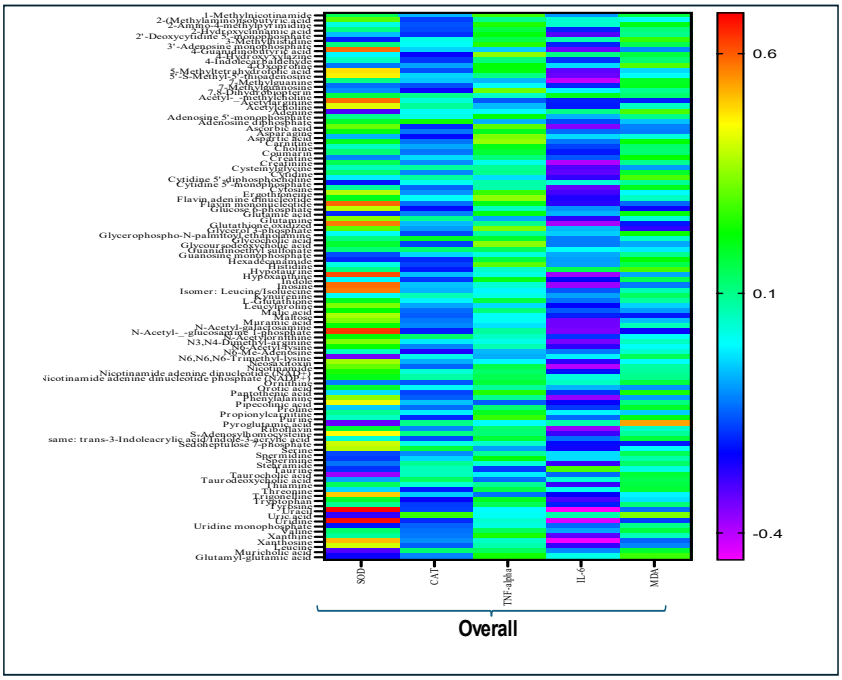

SUPPLEMENTARY FIGURE 1. Heatmap illustrates the correlation between liver metabolites and parameters, including inflammatory markers (TNF-α, IL-6), antioxidant enzymes (SOD, CAT), and lipid peroxidation markers (MDA). Correlation coefficients were computed using Spearman's rank correlation. The heatmap uses a rainbow colour gradient to represent correlation coefficients (r-values). Yellow to red hues represent strong positive correlations, while blue to purple tones indicate strong negative correlations. Green shades reflect weak or negligible correlations

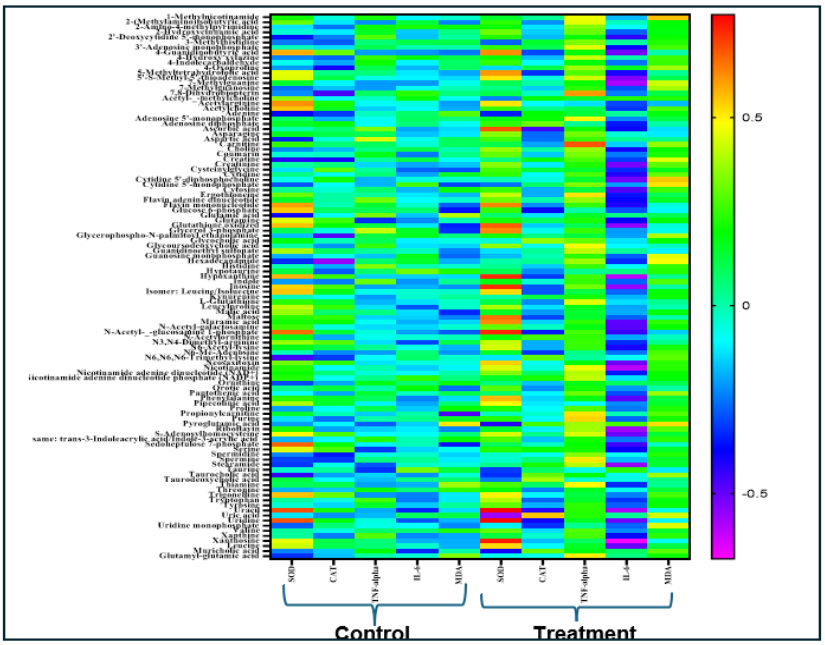

SUPPLEMENTARY FIGURE 2. Heatmap of control and treatment-specific correlations between liver metabolites and all the parameters, including inflammatory markers (TNF-α, IL-6), antioxidant enzymes (SOD, CAT), and lipid peroxidation markers (MDA). Correlation coefficients were computed using Spearman's rank correlation. The heatmap uses a rainbow colour gradient to represent correlation coefficients (r-values). Yellow to red hues represent strong positive correlations, while blue to purple tones indicate strong negative correlations. Green shades reflect weak or negligible correlations

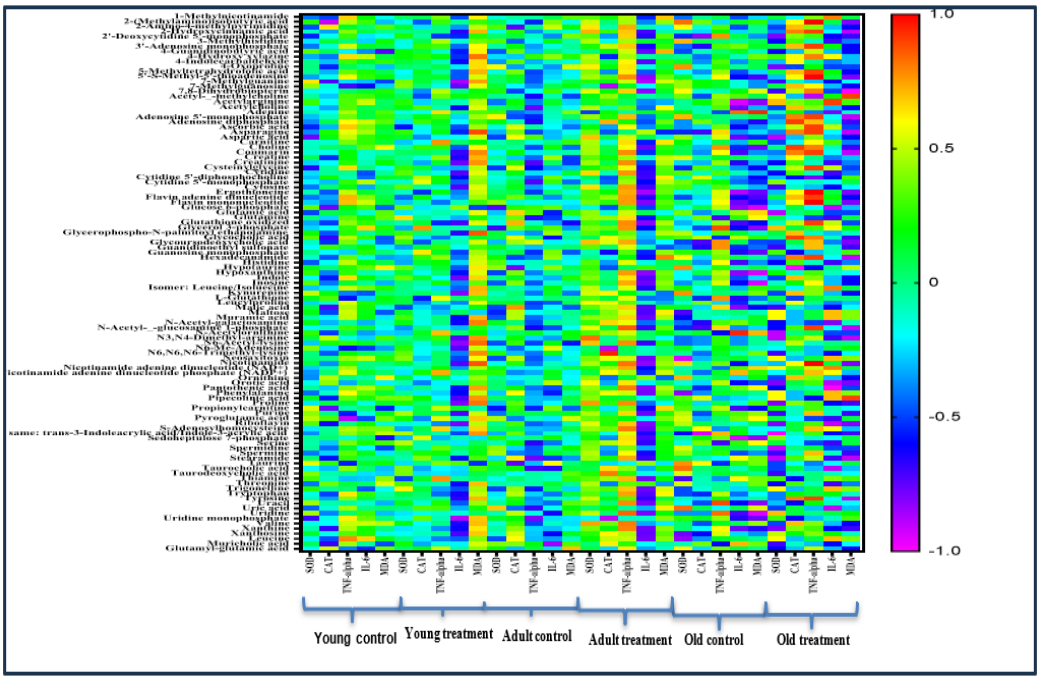

SUPPLEMENTARY FIGURE 3. Heatmap of correlations between liver metabolites and all the parameters including inflammatory markers (TNF-α, IL-6), antioxidant enzymes (SOD, CAT), and lipid peroxidation markers (MDA) in each group. Correlation coefficients were computed using Spearman's rank correlation. The heatmap uses a rainbow colour gradient to represent correlation coefficients (r-values). Yellow to red hues represent strong positive correlations, while blue to purple tones indicate strong negative correlations. Green shades reflect weak or negligible correlations

SUPPLEMENTARY TABLE 1. List of biochemical pathways of significant metabolites profiled for YC vs AC

Pathway name	P	Impact
Valine, leucine and isoleucine biosynthesis	0.025607	0
Taurine and hypotaurine metabolism*	0.025607	0.42857
Lysine degradation	0.093332	0
Arginine and proline metabolism	0.11113	0
Valine, leucine and isoleucine degradation	0.12284	0
Amino sugar and nucleotide sugar metabolism	0.12865	0.00771
Primary bile acid biosynthesis	0.14018	0.02239

*Considered as significant biochemical pathway, p-value <0.05 and impact value > 0.1

SUPPLEMENTARY TABLE 2. List of biochemical pathways of significant metabolites profiled for YC vs OC

Pathway name	P	Impact
Pyrimidine metabolism	0.0058975	0.09246
Pantothenate and CoA biosynthesis	0.063031	0
beta-Alanine metabolism	0.066097	0
Pentose phosphate pathway	0.072205	0.06884
Arginine and proline metabolism	0.11113	0
Amino sugar and nucleotide sugar metabolism	0.12865	0.00771

SUPPLEMENTARY TABLE 3. List of biochemical pathways of significant metabolites profiled for AC vs. AT

Pathway name	P	Impact
Glyoxylate and dicarboxylate metabolism	0.0058988	0
Nitrogen metabolism	0.023069	0
Arginine biosynthesis	0.053135	0.12234
Butanoate metabolism	0.056839	0
D-Amino acid metabolism	0.056839	1
Histidine metabolism	0.06053	0
Citrate cycle (TCA cycle)	0.075176	0.04412
Pyruvate metabolism	0.086035	0.0283
Glutathione metabolism	0.1039	0.01966
Alanine, aspartate and glutamate metabolism	0.1039	0.19712
Porphyrin metabolism	0.11447	0
Arginine and proline metabolism	0.13187	0
Pyrimidine metabolism	0.14217	0.03985
Tryptophan metabolism	0.14898	0.14305
Amino sugar and nucleotide sugar metabolism	0.15237	0.00771